Oblique Waves Lift the Flapping Flag

Jérôme Hœpffner[1,*] and Yoshitsugu Naka[2]

[1]UPMC Univ Paris 06, UMR 7190, Institut Jean Le Rond d'Alembert, F-75005 Paris, France
[2]Ecole Centrale de Lille, Laboratoire de Mécanique de Lille, Boulevard Paul Langevin, 59655 Villeneuve d'Ascq, France

(Received 6 August 2011; revised manuscript received 16 September 2011; published 3 November 2011)

The flapping of the flag is a classical model problem for the understanding of fluid-structure interaction: How does the flat state lose stability? Why do the nonlinear effects induce hysteretic behavior? We show in this Letter that, in contrast with the commonly studied model, the full three-dimensional flag with gravity has no stationary state whose stability can be formally studied: The waves are oblique and must immediately be of large amplitude. The remarkable structure of these waves results from the interplay of weight, geometry, and aerodynamic forces. This pattern is a key element in the force balance which allows the flag to hold and fly in the wind: Large amplitude oblique waves are responsible for lift.

DOI: 10.1103/PhysRevLett.107.194502 PACS numbers: 47.35.−i, 46.40.Jj

When asked to draw a flapping flag, most—scientists and laymen alike—will produce something in the spirit of Fig. 1(a): propagating waves with vertical crests. Figure 1(f) is a typical flag as you could observe on a windy day: The waves are oblique.

In 1879, Lord Rayleigh—Nobel prize laureate and one of the founding fathers of hydrodynamic stability—touches upon the flapping of flags and sails in his influential paper on unstable fluid motion [1]. The analogy between a flag and shear layer stability is immediate since Helmholtz and Kelvin have developed a framework for stability analysis based on surfaces of discontinuity now known as vortex sheets [2,3]. The fluid motion of a shear layer consists of two semi-infinite bodies of constant velocities separated by such an immaterial mobile surface. Quantifying the motion of this surface under the dynamic pressure forces is instrumental in the description of the Kelvin-Helmholtz instability. When this moving surface is bestowed with the additional physical properties of mass, tension, and rigidity, we have the flag. This conception of a flag has inherited the simplifications which are relevant for the description of the Kelvin-Helmholtz instability: It is infinitely long to allow for description of its motion into harmonic waves, and it is two-dimensional with waves propagating with the stream.

The stability analysis for waves short with respect to the flag length has now reached a standard [4]: Applied tension, be it external or induced from fluid drag, is stabilizing, as is bending rigidity, whereas instability increases for longer wavelengths and heavier cloth. The simulations in Ref. [5] confirm the relevance of this local stability analysis for two-dimensional soft flags. Large amplitude analysis shows in addition an hysteretic behavior which is now understood as typical for these systems. This was shown, for instance, in Ref. [6] by observation of the flapping of a silk thread in a falling soap film.

When, on the other hand, considering more rigid media, like a cardboard flag for which the rigidity is such that only waves of length comparable to that of the flag can be unstable [7,8], we see that the dynamics of the vorticity in the free wake will be important for the stability: The flapping induces shedding of vortices, and these vortices act in turn through the pressure on the surfaces of the flag such as to organize a synchronized flapping behavior reminiscent of typical fluid-structure instabilities like aeolian tones [9,10] or airplane wing flutter [11]. For a review of flapping and bending bodies in fluid flow, see [12].

These studies are instrumental steps in conceiving a fundamental model system—as simple as possible—to form the basis of understanding of fluid-flexible structure interaction. We may now take the occasion to turn back to the original inspiration of the flag and see whether the picture is complete or if the simplifications that were made necessary by the search for a quantitative modeling have overlooked some characteristic phenomena. In this, the most striking observation is made by Ref. [13] in a

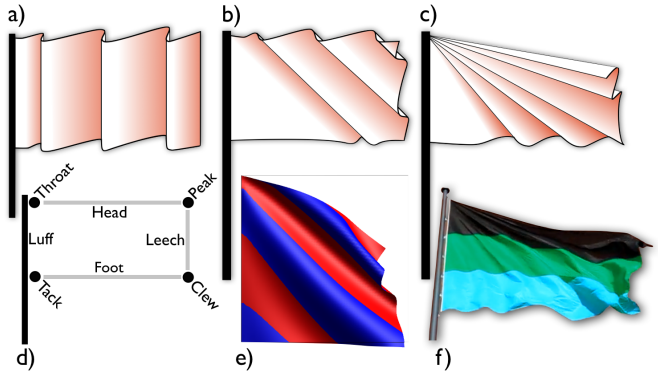

FIG. 1 (color online). General representation of the flag which is discussed in the Letter. (a) Popular conception of the flapping flag with vertical wave crests. (b) A first pattern of oblique waves. (c) An alternative pattern of accordion waves. (d) Naming of the flag's parts in analogy to quadrangular sails. (e) Numerical simulation of a flag in the wind by Ref. [13]. (f) A flapping flag on a windy day.

numerical simulation, showing that the same flag in the same wind remains flat if weightless but flaps with oblique waves otherwise. For another observation of oblique waves in numerical simulations, see [14].

The flag is a piece of cloth held in the wind just like sails are. We may, inspired by Ref. [15], name its elements in analogy to quadrangular sails. See Fig. 1; the leading and trailing edges are the *luff* and the *leech*, the top and bottom edges are the *head* and the *foot*; the top and bottom corners at the pole are the *throat* and the *tack*, and the top and bottom free corners are the *peak* and the *clew*, respectively; see [16,17].

Wave obliquity is of geometrical origin. Consider first the case sketched in Fig. 2(a): no wind—we just distort the rectangular piece of cloth by bringing the leech down; the lower free edge must shorten, and, since the length of the cloth is constant, it wrinkles. These wrinkles connect the throat to a wavy foot and naturally form an oblique pattern. We could in a first step think of the flag's undulation as these wrinkles, advected with the wind along the flag. This wave can grow in amplitude while propagating if instability is strong or decays otherwise.

This first mechanism is really a simplified configuration; let us consider the effect of aerodynamic forces in addition to the cloth weight. Fluid drag generates a tension mitigating the instability, but it is also the only force which can oppose collapse due to weight. The complete surface of the cloth is subject to an oblique force composed of the downward weight and the backward drag as sketched in Fig. 2(b). It is clear that horizontal drag can only partly oppose the weight, but it is not easy to determine which is the exact zone of the flag that will be able to hold flat. On the other hand, we may imagine an analog configuration for which the answer is straightforward. This is the case for

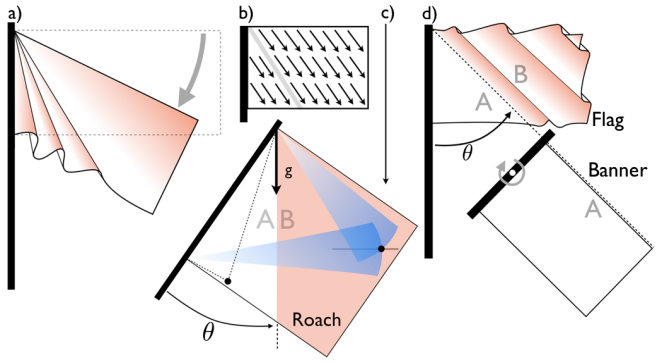

FIG. 2 (color online). Geometrical justification of the oblique waves. (a) Oblique pattern obtained by geometrical deformation of the cloth. (b) Sketch of the oblique surface force applied on the cloth: weight plus fluid drag. (c) Analogy with a tilted cloth and definition of the roach: zone B, which would collapse under the cloth weight. (d) Oblique pattern of waves resulting from the collapse of the roach and comparison with a banner aligned with the external oblique force such that no roach is created.

a flag hanging under its weight only but from a tilted pole as in Fig. 2(c). It is then clear that part B will not hold flat but shall fold and hang below the throat. Indeed, the downward motion of any point of the cloth is constrained by inextensibility, most importantly from the tack and throat whose constraining effect is represented by arcs of circles. Inextensibility forbids any A point to move down, but all B points may through a downward motion reduce the potential energy, so they will. For a true cloth, a slight bending rigidity and the associated elastic energy will partly oppose folding. Now see Fig. 2(d), for the flag put back in the wind. We must expect just the same: Zone B folds or wrinkles, and these wrinkles are advected with the wind and the flag undulates with oblique waves.

The shape of sails is seldom a perfect triangle; sailmakers add an arc of extra material on the leech, called the *roach* [16]. By analogy with this part of the sail which is not directly held between mast and boom, we may call zone B the flag's roach. Also, the frontier may be called the *roach line* and θ the roach angle.

We have here introduced a useful notion: As long as the roach line passes through the cloth—as long as there is a roach—there is no basic stationary flat state whose stability can be formally studied; the roach must collapse and will remain subject to endless flapping. There is no roach if the cloth is cut below the roach line in a triangle shape or if the pole is tilted. If so, there is in fact a stationary state, and assessment of its stability under aerodynamic forces is relevant. If bending rigidity is imparted to the cloth, the flat configuration becomes a stationary state and the roach is unstable to buckling under its own weight.

Note also that we have not considered aerodynamic stability in this discussion: The roach shall fall and fold whatever the instability as predicted by the weightless linear analysis. If the two-dimensional equivalent flag were in addition unstable, the gravity collapse of the roach would be there to feed the motion: Indeed, instability is merely the process by which *preexisting waves* may grow in amplitude. We know now where the preexisting waves may come from.

Advertising banners towed by airplanes are a useful illustration of the above conception. The banners carry no wave, which would otherwise form a great hazard for the flight. Along with our analysis, the main missing ingredient for flutter is here the absence of a pole holding the front of the cloth vertical: no geometrical cause for wave nucleation. The force balance on the cloth—aerodynamic and weight—will naturally align the free banner with the roach line as in Fig. 2(d).

This notion of a roach, central to our purpose, must be certified through a quantitative analysis. We first consider the case of a laminar flow. The average viscous drag per unit surface on a flat plate is $f = 1.3\,\mathrm{Re}^{-1/2}\rho U^2$ [5,18], where the Reynolds number $\mathrm{Re} = \rho UL/\mu$ is based on flag length L and fluid viscosity μ and density ρ. We obtain the

angle θ from the pole by using the balance of cloth weight and viscous pull:

$$\tan(\theta) = \frac{f}{\lambda g} = 1.3\,\mathrm{Re}^{-1/2}\frac{\rho U^2}{\lambda g} = 1.3\,\mathrm{Re}^{-1/2}\frac{\mathrm{Fr}^2}{r} \quad (1)$$

with λ the cloth density, $r = \lambda/\rho L$ the cloth-fluid density ratio, and the Froude number $\mathrm{Fr} = U/\sqrt{gL}$. We compare this formula for the roach angle and thus the wave obliquity with data from Ref. [13]. We have four cases with gravity at our disposal, with $\mathrm{Re} = 200$, $\mathrm{Fr} \in [1, \sqrt{5}]$, and $r \in [0.2, 1]$. We measure θ on these simulated data by coloring the cloth according to the sign of its deflection, as shown in Fig. 1(e), and recording the largest and smallest angles of the waves upstream of the bulge that forms when the cloth folds down at low wind velocities. Case (4) shows the best agreement, which behaves closest to what we expect in our theoretical description of the roach: a moderate transverse deformation and a well-defined pattern of propagative waves rather than a bulge of folds.

For large Reynolds numbers, the flow quickly becomes turbulent. The turbulent boundary layer on both sides of a flat plate exerts an average drag $f = 0.072\,\mathrm{Re}^{-1/5}\rho U^2$ [18], which leads to a roach angle

$$\tan(\theta) = 0.072\,\mathrm{Re}^{-1/5}\frac{\rho U^2}{\lambda g}. \quad (2)$$

We performed a set of wind tunnel experiments using a 0.6×0.6 m^2 silk flag of density $\lambda = 42$ g/m^2 ($r \simeq 0.06$). The cloth is clamped to a vertical wire by using Scotch tape, and its motion is recorded from the side by using a high speed camera. The wave activity can be appreciated from the shadow-reflection pattern of an halogen lighting below and upstream of the flag. The wind speed U is measured by using a Pitot tube upstream of the test section. Figure 3(b) displays the smallest and largest wave angles obtained from the video sample by measuring the straight shadow lines originating at the luff and extending across the flag.

The mere turbulent boundary layer pull of Eq. (2), shown with a dashed line, largely underpredicts the wave angle. We know, on the other hand, that in fluid-structure instabilities onset of flutter induces a larger drag. A theoretical analysis was done for the case of a flapping flag in Ref. [15], and measurements were performed in Ref. [19] for a flag under longitudinal tension. In Fig. 9 of Ref. [19], the drag of a fluttering polyethylene sheet is displayed with comment that "the measured results indicate that the drag experienced by the flag is generally of $\mathcal{O}(10)$ greater than that of a plate of equal dimensions." The theoretical roach angle with that magnified force is drawn as a solid line, and we observe that the order of magnitude of the angle is now much better.

This example shows that the mere viscous drag of a high Reynolds number flow fails to have the flag fly. We have justified the presence of oblique waves, so we may now discuss three mechanisms by which obliquity will impart the flag with aerodynamic *lift*. Here we denote by lift the component of aerodynamic force which opposes weight and by drag the component in the wind direction.

Finite amplitude waves nucleate free vortices and recirculation zones. This large scale unsteadiness induces through pressure forces across the cloth a drag much larger than that of viscous shear. In Ref. [15], it is shown that, against the usual conception, a structural aspect of the large wave motion may also be responsible for large tension due to the in-plane back and forth motion of the cloth. These are the effects we invoked to predict a realistic wave angle in Fig. 3(b). In Ref. [19], the force from the unsteady motion of a flapping flag was measured only horizontally,

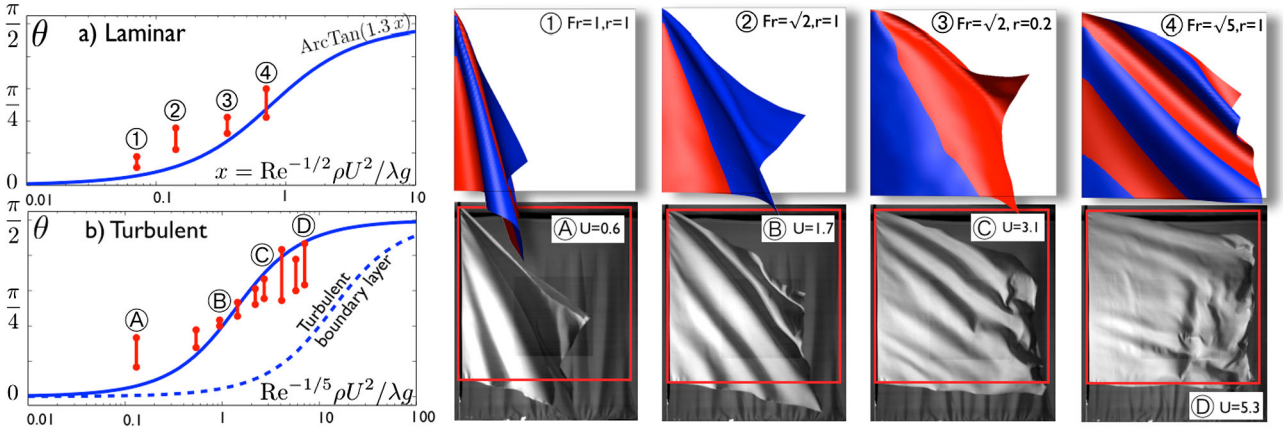

FIG. 3 (color online). Measurement of the wave angle. (a) Low Reynolds number; the wave angle obtained by a balance of aerodynamic drag and weight for a laminar flow from Eq. (1), compared to numerical simulations from Ref. [13]. The flag is colored in blue (red) for positive (negative) deflections of the cloth. (b) High Reynolds number; wave angle estimated from turbulent boundary layer drag using Eq. (2) (dashed line) and with a force magnified to account for extra drag due to large amplitude wave motion (solid line). The flag motion is shown in a movie included as Supplemental Materials [21].

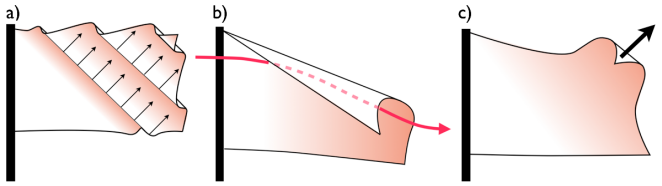

FIG. 4 (color online). Three causes of lift due to oblique waves. (a) Aerodynamic resistance due to a large wave amplitude. (b) Lift through downpush of the stream. (c) Lift through snapping at the peak.

but in fact the aerodynamic force must be orthogonal to the wave's crest and induces lift as sketched in Fig. 4(a).

This first lift is a mere modification of the effect already known for vertical waves. A new effect is found in the downward deflection of streamlines. The situation is best illustrated in Fig. 4(b) by an exaggeration of the oblique pattern, here just formed of the head and peak flipping and folding over. We observe this motion dominant at low wind velocities. The flipping of the upper part of the flag in a wide coherent motion provides a large lifting surface. This situation must be unsteady: The cloth slips along the deflected stream and flips over to the other side in a periodic motion.

We may invoke yet a third mechanism for lift through a phenomenon analog to the crack of the whip [20]. This is discussed for flags in Ref. [5] as a "snapping event." When large waves propagating along the cloth reach the leech, the kinetic energy stored up is focused through reflection at the free boundary and induces a fast flip of the tip: the snap, responsible for quick and large tension event, which peaks at about 5 times the average pull. Now through obliquity, this snapping is directed upward at the peak as sketched in Fig. 4(c), and we may speculate that the snapping at a corner would be even more violent through focusing onto a smaller area. We note that the peak is typically where old flags show most wear.

Now that we have introduced the additional forces due to the presence of the waves, we may think of a wave configuration in a pattern of an accordion linked to the throat as illustrated in Fig. 1(c). Through the magnified pull, all points at the cloth are strongly dragged away from the pole, aft, and up. The configuration most compatible with this pull and the weight is a downward rotation of beams stemming from the throat: the accordion wrinkles. Indeed, we observe this pattern in the photograph of Fig. 1(f) but in a motion of lesser coherence with erratic connections and dissolution of a general pattern of accordion wrinkles. The notion of a roach is still relevant in this configuration to define a region which is not concerned with the gravity collapse, but now the most relevant measure should be the oblique angle of the head, which is linked to the wavelength and the wave amplitude along the cloth.

Oblique waves are omnipresent in the flapping of flags under gravity. We have explored their origin and impact on the ability of the flag to fly in the wind through a lift effect. The roach angle θ is a simple way to describe the wave obliquity. The drag of a flapping flag in turbulent flow conditions was measured in Ref. [19]; it would be very interesting if the lift could be measured as well. We should not be surprised if the scale measured a weight lesser than that of the cloth. In the extreme, the cloth may be entirely carried by the wind. More is impossible since a flag deflected upward would form a reversed oblique pattern of waves [Fig. 2(a), flipped], and the vertical force we have described would then push the flag back down to horizontal.

We are grateful to Professor Hyung Jin Sung and Wei-Xi Huang of Ref. [13], who were kind to share their data for comparison, and to Professor Howard Stone for an encouraging discussion during his stay at the lab. We could use the wind tunnel and high speed camera at the Laboratoire de Mécanique de Lille thanks to Professor Michel Stanislas.

*jerome.hoepffner@upmc.fr

[1] Lord Rayleigh, Proc. London Math. Soc. **s1-10**, 4 (1878).
[2] H. Helmholtz, Philos. Mag. Ser. 4 **36**, 337 (1868).
[3] W. Thomson, Philos. Mag. Ser. 4 **42**, 362 (1871).
[4] M. P. Païdoussis, *Fluid-Structure Interactions: Slender Structures and Axial Flow* (Academic, New York, 1998).
[5] B. S. H. Connell and D. K. P. Yue, J. Fluid Mech. **581**, 33 (2007).
[6] J. Zhang, S. Childress, A. Libchaber, and M. Shelley, Nature (London) **408**, 835 (2000).
[7] M. Argentina and L. Mahadevan, Proc. Natl. Acad. Sci. U.S.A. **102**, 1829 (2005).
[8] C. Eloy, R. Lagrange, C. Souilliez, and L. Schouveiler, J. Fluid Mech. **611**, 97 (2008).
[9] Lord Rayleigh, Philos. Mag. Ser. 6 **29**, 433 (1915).
[10] J. Jeans, *Science and Music* (Dover, New York, 1968).
[11] T. Theodorsen, NACA Technical Report No. 496, 1935.
[12] M. J. Shelley and J. Zhang, Annu. Rev. Fluid Mech. **43**, 449 (2011).
[13] W.-X. Huang and H. J. Sung, J. Fluid Mech. **653**, 301 (2010).
[14] Y. Kim and C. S. Peskin, Phys. Fluids **19**, 053103 (2007).
[15] P. M. Moretti, Int. J. Acoustics Vib. **8**, 227 (2003).
[16] D. Seidman, *The Complete Sailor: Learning the Art of Sailing*, International Marine Series (McGraw-Hill, New York, 2011).
[17] C. A. Marchaj, *Sail Performance: Theory and Practice* (Adlard Coles Nautical, London, 1996).
[18] H. T. Schlichting and K. Gersten, *Boundary-Layer Theory* (Springer-Verlag, Berlin, 1999).
[19] M. Morris-Thomas and S. Steen, J. Fluids Struct. **25**, 815 (2009).
[20] T. McMillen and A. Goriely, Physica (Amsterdam) **184D**, 192 (2003).
[21] See Supplemental Material at http://link.aps.org/supplemental/10.1103/PhysRevLett.107.194502 for a movie of the flag with oblique waves.